JCB Article

Dual function of Slit2 in repulsion and enhanced migration of trunk, but not vagal, neural crest cells

Maria Elena De Bellard,[1] Yi Rao,[2] and Marianne Bronner-Fraser[1]

[1]Division of Biology, California Institute of Technology, Pasadena, CA 91125
[2]Department of Anatomy and Neurobiology, Washington University School of Medicine, St. Louis, MO 63110

Neural crest precursors to the autonomic nervous system form different derivatives depending upon their axial level of origin; for example, vagal, but not trunk, neural crest cells form the enteric ganglia of the gut. Here, we show that Slit2 is expressed at the entrance of the gut, which is selectively invaded by vagal, but not trunk, neural crest. Accordingly, only trunk neural crest cells express Robo receptors. In vivo and in vitro experiments demonstrate that trunk, not vagal, crest cells avoid cells or cell membranes expressing Slit2, thereby contributing to the differential ability of neural crest populations to invade and innervate the gut. Conversely, exposure to soluble Slit2 significantly increases the distance traversed by trunk neural crest cells. These results suggest that Slit2 can act bifunctionally, both repulsing and stimulating the motility of trunk neural crest cells.

Introduction

Neural crest cells emerge from the dorsal neural tube and migrate along pathways that are characteristic of their axial level of origin, with cells from different axial levels populating different derivatives (Le Douarin, 1986; Bronner-Fraser et al., 1991; Le Douarin et al., 1992). For example, vagal neural crest cells emerge from the caudal hindbrain and migrate into and along the rostrocaudal extent of the gut where they form the enteric ganglia. In contrast, trunk neural crest cells never enter the gut, even if transplanted to vagal levels (Le Douarin and Teillet, 1973, 1974; Erickson and Goins, 2000). Little is known about the molecular mechanisms underlying these differences in the migratory pathways taken by trunk and vagal neural crest cells.

Several inhibitory molecules have been shown to play important roles in neural crest migration. For example, ephrinB family members prevent neural crest entry into the caudal portion of each somite, resulting in segmental migration in the trunk region (Krull et al., 1997; Wang and Anderson, 1997). Other molecules implicated in neural crest cell guidance include chondroitin sulfate proteoglycans (Oakley et al., 1994) and Semaphorin3A and 3C (Eickholt et al., 1999; Brown et al., 2001; Feiner et al., 2001). However, none of these explain differences between the ability of vagal and trunk neural crest populations to enter the gut.

Slit proteins play important roles in axonal guidance in both vertebrates and invertebrates (Brose et al., 1999; Kidd et al., 1999; Li et al., 1999). These glycoproteins are known to be potent chemorepellents for midline axons in *Drosophila* as well as olfactory, forebrain, and dentate gyrus axons in mammals (Brose et al., 1999; Kidd et al., 1999; Li et al., 1999; Nguyen Ba-Charvet et al., 1999; Bagri et al., 2002). Slits function as repulsive factors during migration of neurons and glia (Hu, 1999; Wu et al., 1999; Zhu et al., 1999; Kinrade et al., 2001) and also can regulate axon elongation/branching in mammals (Wang et al., 1999).

In this study, we examine the potential role of Slit in neural crest migration. Slits are expressed in places where they could influence migrating neural crest cells (in the dorsal neural tube from which neural crest cells emigrate and near the entrance to the gut, which is selectively invaded by vagal, but not trunk, neural crest cells). Consistent with this, we find that only trunk neural crest cells possess Robo receptors for Slit. We tested the possible functional role of Slit on neural crest migration in vitro and in vivo by confronting neural crest cells with Slit2-producing cells or soluble Slit2. The results reveal for the first time a dual role for Slit2 in a migratory cell type, both inhibiting movement when in direct confrontation and enhancing motility when in solution. Our results at least partially account for the differential ability of vagal, but not trunk, neural crest cells to invade and innervate the gut.

The online version of this article includes supplemental material.

Address correspondence to Marianne Bronner-Fraser, Division of Biology, 139-74, California Institute of Technology, 1200 East California Blvd., Pasadena, CA 91125. Tel.: (626) 395-3355. Fax: (626) 395-7717. E-mail: mbronner@caltech.edu

Key words: Slit2; neural crest; vagal; chemorepellent; gut

The Journal of Cell Biology, Volume 162, Number 2, July 21, 2003 269–279
http://www.jcb.org/cgi/doi/10.1083/jcb.200301041

Supplemental Material can be found at:
http://www.jcb.org/cgi/content/full/jcb.200301041/DC1

Results

Slit and Robo receptor expression during development

We examined the distribution pattern of vertebrate Slits and their Robo receptors at the time of active neural crest migration in chick embryos at embryonic days 2 and 3. Both whole mount and section in situ hybridization were performed for transcripts encoding Slits 1, 2, and 3 as well as Robo1 and Robo2.

We found that the patterns of expression for Slit2 (Fig. 1, a, d, and e), Slit1 (Fig. 1, b and c), and Slit3 (Fig. 1 f) largely overlapped. All were expressed prominently in the splanchnic mesoderm that marks the entrance to the gut. In addition, there was marked expression in the ventral neural tube, notochord, and dorsomedial dermomyotome. Slit1 and Slit2 were expressed strongly in the roof plate, whereas Slit3 had little or no expression in this site. Interestingly, Slit1 and Slit2 were expressed in both the floor plate and in forming motor neuron pools. In contrast, Slit3 was expressed in motor neurons but had low expression in the floor plate. These expression patterns are similar to those noted previously in the mouse (Yuan et al., 1999).

Trunk, but not vagal, neural crest cells express both Robo1 and Robo2 receptors (Figs. 2 and 3). Whole mount in situ hybridization reveals Robo receptors on neural crest cells as they migrate through the trunk somites (Fig. 2, a–c, e, and g). However, neural crest cells at vagal levels, which can be visualized by their expression of the HNK-1 epitope (Fig. 2 f), lack detectable Robo receptors. Robo1 expression was similar to that of Robo2 but initiated at later stages. By section in situ hybridization, which gives better cellular resolution, we noted that Robo1 (Fig. 3, a and b) and Robo2 (Fig. 3, c and d) were expressed on migrating trunk neural crest cells. In contrast, vagal neural crest cells lacked Robo receptor expression above background (Fig. 3, e–h). Not all HNK-1$^+$ migrating trunk neural crest cells were Robo$^+$ during early stages of migration. With developmental age, the levels of Robos on migrating neural crest cells appeared to increase such that late migrating trunk neural crest cells expressed high levels of both receptors (see Fig. S1, available at http://www.jcb.org/cgi/content/full/jcb.200301041/DC1). In addition to the neural crest, Robo1 is seen in motor neurons. Robo2 appears throughout the neural tube with the exception of the ventral-most region. All Robos are expressed at low levels in the dermomyotome. These observations confirm and extend previous work by others in mouse (Holmes et al., 1998; Yuan et al., 1999) and chick embryos (Li et al., 1999; Holmes and Niswander, 2001; Vargesson et al., 2001).

Trunk, not vagal, neural crest cells are repelled by Slit2

We next examined the effect of vertebrate Slit on neural crest migration in vivo and in vitro using Slit2 as a ligand for most experiments. The expression patterns and functions of Slits have been shown to overlap in other published assays (Wu et al., 1999; Bagri et al., 2002), and we verified that Slit1 can function similarly to Slit2 (see below).

Cells expressing Slit2 were introduced onto neural crest migratory pathways. HEK293 cells transfected either with human Slit2 or control vectors (Li et al., 1999) were labeled with DiI and microinjected onto trunk and/or vagal neural crest migratory pathways in early chick embryos. Vagal level injections were performed into somites 1–7 of stage 10–12 chicken embryos (Hamburger and Hamilton, 1951). When injected into this location, the labeled cells appeared to localize in ventral sites around the dorsal aorta, as has been previously described for injections of cells or latex beads (Bronner-Fraser and Cohen, 1980; Bronner-Fraser, 1982). Vagal neural crest cells migrate from the neural tube and proceed ventrally to populate the dorsal root and sympathetic ganglia. Other vagal crest cells migrate further ventrally to penetrate the gut. When encountering Slit2-secreting cells at the level of the aorta, the vagal neural crest cells appeared to mix and closely associate with Slit2-secreting cells (Fig. 4, c–e). Their distribution pattern was similar to that observed after injection of parental control cells (Figs. 4, a and b). Little or no avoidance behavior was observed after either injection of Slit2 cells (n = 1/8 embryos) or control cells (n = 0/6 embryos) at vagal levels.

In marked contrast to injections at vagal levels, when Slit2-expressing cells were introduced onto trunk neural crest migratory pathways at the level of somites 8–28 in stage 12–16 embryos, the trunk neural crest cells avoided and circumvented the Slit2-expressing cells. In whole mount view, neural crest cells appeared to stop when confronted by an aggregate of Slit2-expressing cells (Fig. 4, f–l). The injected cells were localized ventrally adjacent to the aorta, which is a site normally populated by neural crest cells. Although trunk neural crest cells approached the vicinity of the Slit2-expressing cells, they failed to contact and mix with them and were generally distant by one cell diameter or more (Fig. 4, f, j, and l), whereas they freely intermixed with control cells (Fig. 4 h). Avoidance behavior was observed after injection of Slit2 cells (n = 12/15 embryos) but rarely after injection of control cells (n = 1/10 embryos) at trunk levels.

To visualize the interaction between neural crest cells and Slit2-expressing cells, we turned to an in vitro system in which cultured neural crest cells were confronted with Slit2-expressing cells. Neural tubes containing premigratory neural crest cells were isolated from stage 13–16 embryos and plated onto tissue culture dishes in close proximity to control or Slit2-expressing cells. In this way, delaminated neural crest cells emerged from the neural tube and migrated toward the Slit2-expressing cells in a two-dimensional environment. After each experiment, cultures were stained with the HNK-1 antibody to confirm that the migrating cells were neural crest cells. Under these conditions, ~90% of the migrating cells were HNK-1 positive.

Whereas trunk neural crest cells freely approached and intermixed with control HEK cells (Fig. 5 a), a sharp border was observed between trunk neural crest cells and Slit2-expressing cells (Fig. 5 b). A similar experiment was performed for vagal neural crest cells, using neural tubes explanted from the levels of somites 1–7 of stage 10–12 embryos. In this case, the vagal cells intermixed equally well with Slit2-expressing cells and control cells (Figs. 5, c and d). Thus, analogous differences in the response of trunk versus vagal neural crest cells were noted both in vivo and in vitro, suggesting that the former, but not the latter, avoided an exogenous source of Slit2. Table I summarizes the results for in vivo and in vitro assays.

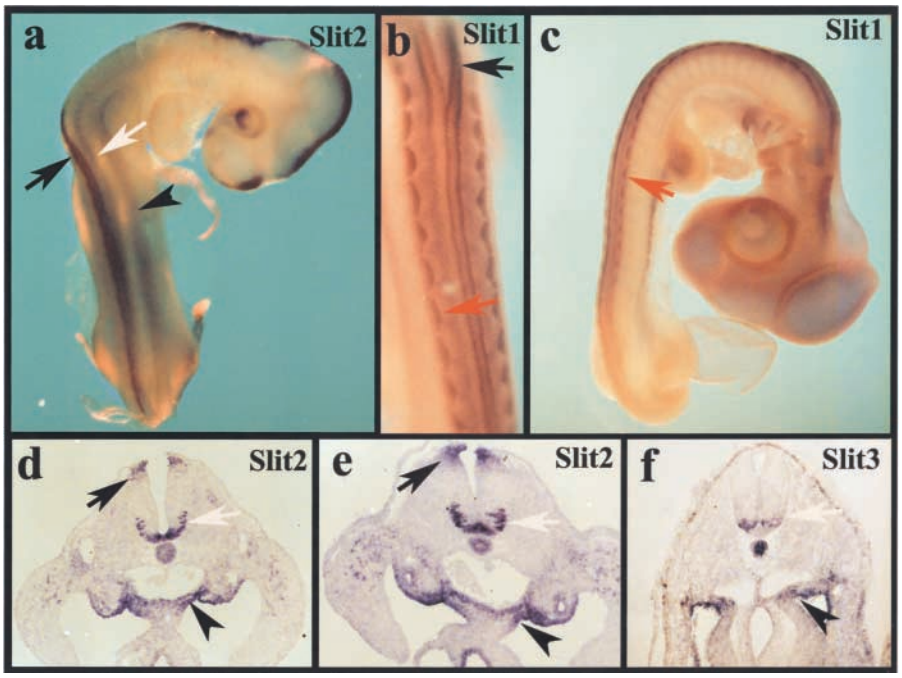

Figure 1. **Expression of Slits during neural crest migration.** In situ hybridization of Slit2, 1, and 3 demonstrates that Slits are expressed in the mesenchyme at the entry to the gut as well as in the neural tube and somites. (a–c) Whole mounts of stage 17 chicken embryos. (a) Whole mount in situ hybridization with a Slit2 probe reveals that it is expressed in the dorsal neural tube (black arrow), ventral neural tube (white arrow), and gut mesenchyme (black arrowhead). (b and c) Whole mount in situ hybridization with a Slit1 probe reveals that it is expressed in the dorsal neural tube, dorsomedial dermomyotome (red arrow), and gut mesenchyme. (b) A higher magnification of c. (d) Transverse section in situ hybridization through the lumbar level of a stage 17 chick embryo shows Slit2 in the floor plate and developing motor neurons (white arrow), the roof plate of the neural tube (black arrow), and the mesenchyme immediately dorsal to the gut (black arrowhead); the Slit1 pattern (not depicted) looked identical. (e) A similar expression pattern for Slit2 and Slit1 (not depicted) was observed at the hindlimb level of a stage 19 embryo. (f) Slit3 in a stage 16 embryo appeared similar to the other Slits, except that staining was reduced or absent in the floor plate and dorsal neural tube.

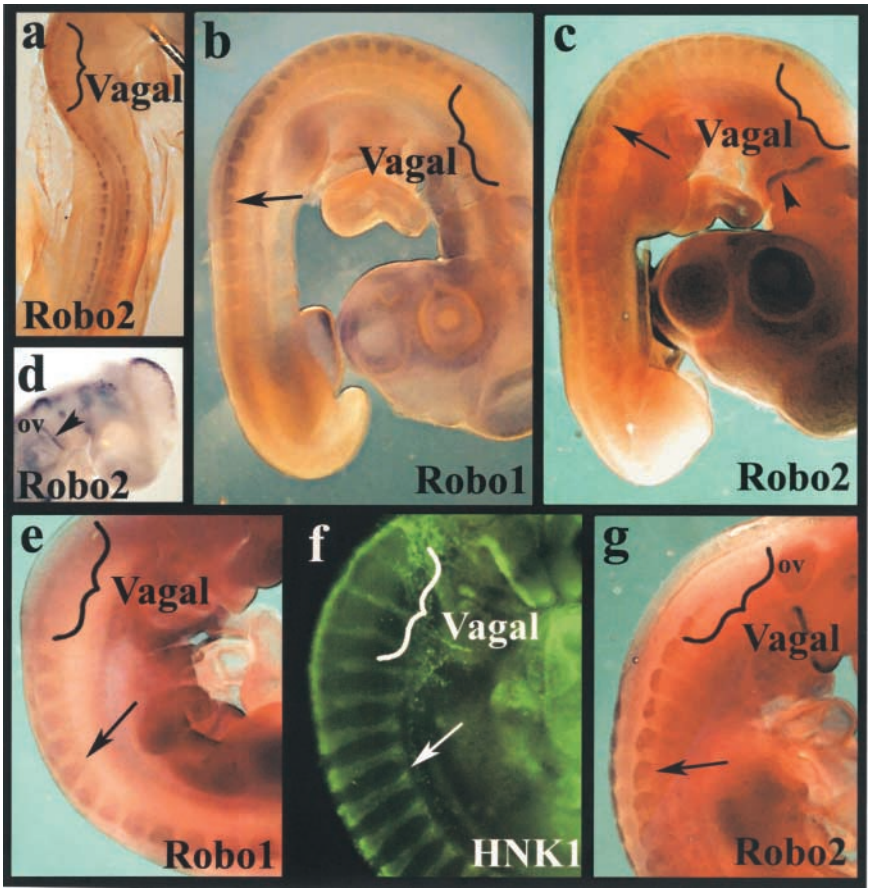

Figure 2. **Expression of Robos during neural crest migration.** Whole mount in situ hybridization with Robo1 and Robo2 probe reveals that the receptor is expressed in the trunk neural tube, on migrating trunk neural crest cells within the somites, and in the dermomyotome, but is not expressed by vagal neural crest cells. (a) In a stage 15 chicken embryo, there is no staining for Robo2 at vagal levels (bracket) though there is staining at truncal levels. (b and c) At stage 18 during the peak of neural crest migration, Robo1 (b) and Robo2 (c) are strongly expressed in neural crest cells at the trunk levels (black arrows) but not in the vagal region (brackets). (d) Robo2 labeling in the head of a stage 15 embryo shows staining on the dorsal half of the otic vesicle (ov), trigeminal placode, and dorsal neurons in the mesencephalon; the posterior part of the second/hyoid branchial arch is also positive for Robo2 (arrowhead). (e–g) At stage 20, when neural crest cells are condensing to form the dorsal root ganglia (arrows), Robo1 (e) and Robo2 (g) are strongly expressed in trunk, but not vagal (brackets), regions. (f) The same stage embryo labeled with HNK-1 shows neural crest cells migrating and beginning to condense into dorsal root ganglia at both vagal and trunk levels.

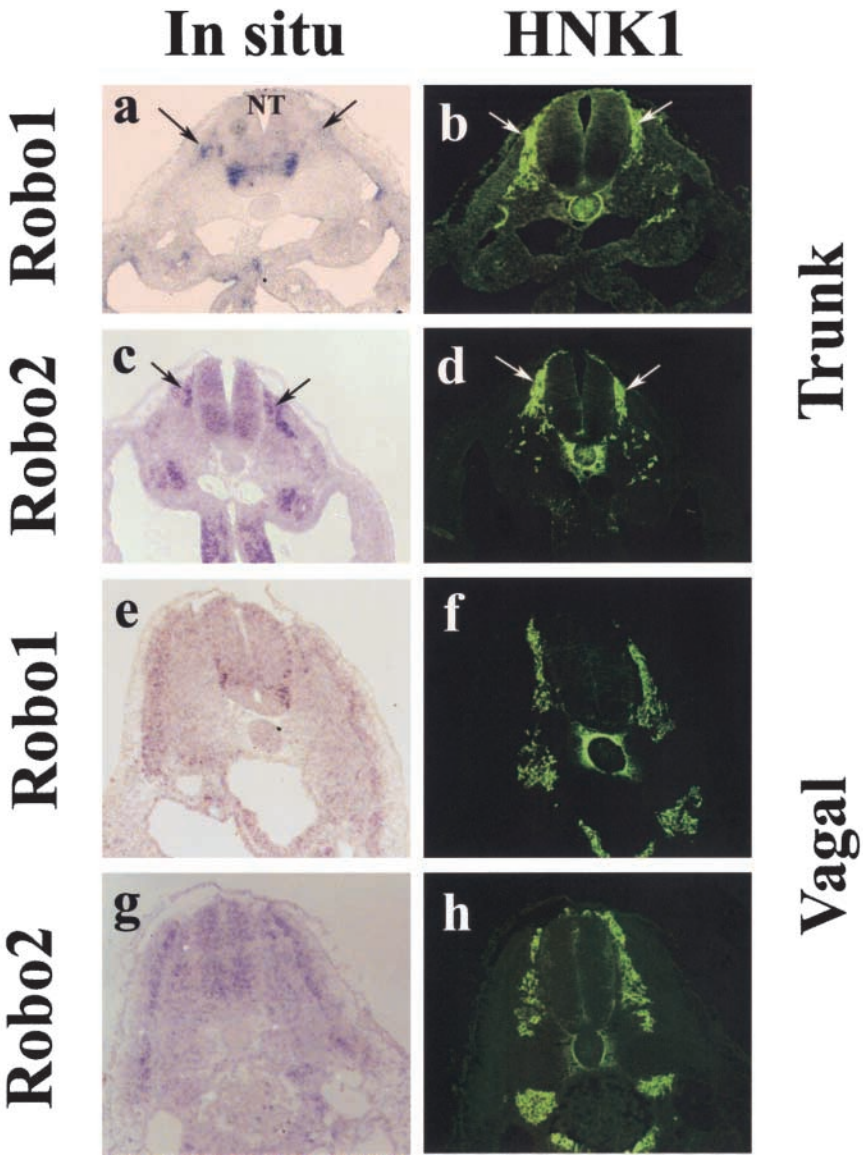

Figure 3. **Expression of Robos on migrating trunk but not vagal neural crest.** Section in situ hybridization with Robo1 and Robo2 probes reveals that the receptor is expressed in the trunk neural tube and on migrating trunk neural crest cells within the somites but is not expressed by vagal neural crest cells. All embryos were stage 18. Left panels show in situ signal, and right panels show the same section stained with HNK-1 antibody to recognize neural crest cells. (a and b) Robo1 is strongly expressed in trunk neural crest cells (arrows) and motor neuron precursors in the ventral neural tube (NT). (c and d) Robo2 is also strongly expressed in migrating trunk neural crest cells and the neural tube, except for the ventral-most side. (e–h) At vagal levels, Robo1 (e and f) and Robo2 (g and h) are expressed in the dermomyotome and neural tube but not in the migrating vagal neural crest cells.

In addition to Slit2, we also tested on trunk neural crest cells the effects of exposure to Slit1-expressing cells using the same in vitro paradigm as described above for Slit2. These results were identical (not depicted), suggesting that Slit1 is also a repellent for trunk neural crest cells.

Slit2 repulsive effect on trunk neural crest is contact mediated

Although Slit2 is soluble and can be secreted, it is most commonly found in membrane extracts and tightly associated with the cell surface (Brose et al., 1999; Nguyen Ba-Charvet et al., 2001a). To determine if the effects of Slit2 on trunk neural crest cells were caused by soluble Slit2 present in the media (Wu et al., 1999) or by cell membrane–associated Slit2 (Hu, 2001; Nguyen-Ba-Charvet et al., 2001b), we repeated the in vitro assay above with cells that were dried and dead but retained membrane-bound Slit2 (not depicted). Under these conditions (Figs. 5, e–h), trunk, but not vagal, neural crest cells avoided Slit2 membrane ghosts, confirming that the effects of Slit2 are cell surface dependent. These results are summarized in Table I.

Soluble Robo reverses Slit2 repulsion of trunk neural crest

Slit2 is a known ligand for the Robo1 and Robo2 transmembrane receptors (Brose et al., 1999). We tested the ability of a soluble form of the receptor to neutralize the effects of exogenous Slit2. RoboN consists of the extracellular portion of Robo1 (Wu et al., 1999). When trunk neural crest cells were grown in media conditioned by the RoboN-secreting cells, the repulsive effect caused by Slit2 was reversed (Table II), suggesting that the effect was indeed Slit mediated. In contrast, RoboN media had no significant effect on trunk crest encountering control HEK cells. Similarly, trunk neural crest cells showed no altered behavior when encountering RoboN-secreting cells alone (not depicted).

Soluble Slit2 affects trunk, not vagal, neural crest migratory properties

The observation that the membrane-bound form of Slit2 appears to be responsible for its chemorepulsive effects on neural crest cells does not rule out a possible function of the soluble

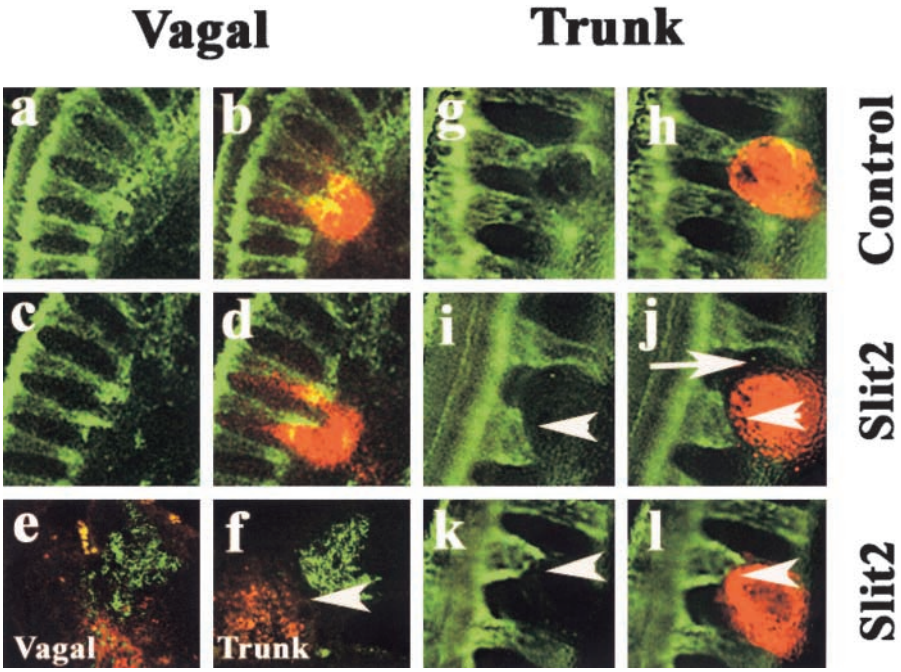

Figure 4. **Effects of Slit2-expressing cells on neural crest migration in vivo.** Cells expressing Slit2 or control HEK cells were labeled with the lipophilic dye DiI and implanted onto vagal and/or trunk neural crest migratory pathways. Left panel shows flattened confocal Z-series of whole mounts of embryos stained with the HNK-1 antibody (green) to recognize neural crest cells, and the right panel shows both the neural crest and the injected cells (red) at both vagal and trunk levels. Embryos were analyzed one day after injection. (a–d) At vagal levels, neural crest cells intermixed with both control and Slit2-expressing cells. (g–l) In contrast, at trunk levels, neural crest cells overlapped with control cells (g and h) but appeared to stop (white arrowhead) some distance away from Slit2 cells (i–l). Notice also how trunk neural crest cells circumvent Slit2-expressing cells (white arrow in j). (e and f) Sections through embryos injected with Slit2 show that vagal neural crest freely intermix with Slit2 cells, whereas trunk neural crest cells avoid (white arrowhead) Slit2 cells.

form of the molecule. In fact, we noted that trunk neural crest cells in the vicinity of Slit2-expressing cells in vivo and in vitro appeared more elongated than in the presence of control cells, raising the possibility that cytoskeletal and/or motility changes may occur in the presence of soluble Slit2.

To examine the effects of soluble Slit2, migrating neural crest cells were placed on fibronectin-coated substrates transfilter to Slit2-expressing cells, control cells, Slit2-conditioned medium (CM),* or control CM (Wu et al., 2001). This assures that crest cells under experimental conditions would be exposed only to the soluble form of Slit2. With either transfilter Slit2 cells or Slit2 CM, the maximum distance traveled by neural crest cells was an average of 21% more than that observed under control conditions ($n > 100$ neural tubes in a total of 12 separate experiments; Table III; Fig. 6). In contrast, vagal neural crest cells failed to exhibit enhanced migration under identical conditions ($n = 12$ neural tubes in a total of three separate experiments; Table III).

*Abbreviations used in this paper: CM, conditioned medium.

Table I. **Trunk, but not vagal, neural crest cells avoid Slit2-expressing cells**

	In vivo		In vitro	
	Control	Slit2	Control	Slit2
Live cells				
Trunk	1/10	12/15	2/12	18/20
Vagal	0/6	1/8	0/6	0/6
Dried cell ghosts				
Trunk			0/5	5/7
Vagal			0/6	0/6

Numbers correspond to individual embryos (in vivo) or neural tubes with migrating neural crest (in vitro) that showed avoidance when encountering either the control or Slit2-expressing cells.

In a second assay for Slit2's effects on migrating neural crest cells, we examined the rapidity with which neural crest cells closed an injury-induced gap within their population (Fig. 7 a). In the presence of Slit2 CM, >20% of cultures had completely sealed the gap within 2 h, compared with <10% of cultures exposed to control medium (Fig. 7 b; Table IV). Moreover, when cells were "primed" with CM before the wound assay, >40% of cultures had sealed the wound within 2 h, compared with <20% of controls ($P < 0.005$; Table IV). The increased migratory response occurred rapidly, within ~1 h of exposure to Slit2. Given this short time interval, an increase in the number of migratory cells is unlikely (Mason et al., 2001). Consistent with this, no increase in cell division was observed by anti-phosphohistone3 labeling, when neural crest cells were exposed to Slit2 (unpublished data). Furthermore, we noted no alteration in cell death, as assayed by pyknotic nuclei identified by DAPI staining (unpublished data). In contrast to trunk neural crest cells, vagal neural crest cells were unaffected by the presence of Slit2 in the medium.

We repeated the wound assay but preexposed the cells to either control or Slit2 CM mixed with RoboN CM (1:1) to see if this reversed the effects of Slit2. RoboN CM reduced ($P < 0.02$) the percentage of cells closing the gap

Table II. **Slit2 repulsion is neutralized by RoboN**

	Explants with inhibition out of total number	
	−RoboN	+RoboN
Control	3/23	1/22
Slit2	16/27	3/22[a]

Neural tubes were cultured overnight on fibronectin-coated slides containing control medium or Slit2 with or without RoboN. Inhibition is defined by the presence of a clear separation between neural crest cells and the Slit2 or control cell lines. Control, untransfected HEK293; Slit2, combined results from two different Slit2-expressing cell lines.
[a]$P < 0.00001$, Chi-squared test.

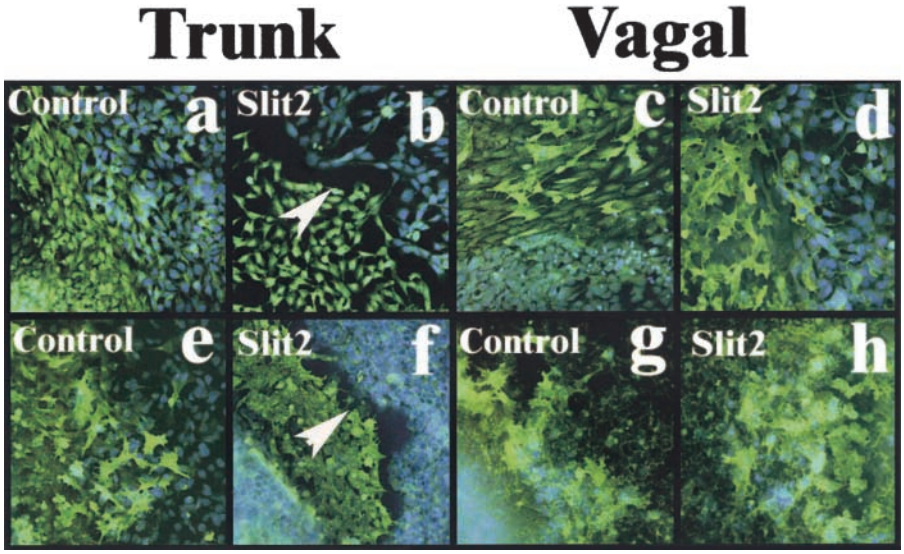

Figure 5. **Trunk, not vagal, neural crest cells are repelled by Slit2-expressing cells in vitro.** (a–d) Trunk and vagal neural crest cells (green) were grown apposed to live control HEK cells (a and c) or Slit2-expressing cells (b and d) (blue DAPI label). Only when trunk neural crest cells (b) were grown with Slit2-expressing cells was there a sharp border (white arrowhead) formed between the two populations. (e–h) A similar experiment performed with dead control or Slit2-expressing cells again shows a border between trunk neural crest cells and the Slit cell ghosts (white arrowhead in f), demonstrating that the repellent activity is membrane bound.

within 2 h by half, a level similar to that observed under control conditions (Fig. 7 c; Table IV).

Slit2 increases trunk neural crest cell motility

The results suggest that soluble Slit2 enhances neural crest migration, as the distance traveled by the cells as a function of time increases significantly. To view this at higher resolution, we tracked individual cell movement by imaging neural crest cells in the presence or absence of soluble Slit2 by time-lapse video microscopy. To aid visualization, trunk neural tubes were electroporated with a GFP expression vector in vivo (Megason and McMahon, 2002), and then the tubes were explanted in vitro. Cultures were primed with Slit2 or control CM and filmed under a confocal microscope. The resultant movies were analyzed to examine the total and net distance navigated, speed, directionality, and persistence of movement of individual, GFP-labeled neural crest cells.

The results confirmed static pictures showing that trunk neural crest cells moved more dynamically and for greater distances in Slit2 than in control medium (Fig. 8; see Videos 1 and 2, available at http://www.jcb.org/cgi/content/full/jcb.200301041/DC1). With or without Slit2, neural crest cells moved in a somewhat erratic manner, with frequent changes in direction (Kulesa and Fraser, 1998, 2000). The cells appeared to collide more frequently in the presence of Slit2, raising the possibility that cell–cell collision may effect their degree of movement.

Fig. 9 a, which illustrates by groups the total path length of all cells normalized to a total of 2.5 h, shows that the Slit2-exposed neural crest cells tend to move further than control-treated cells, with twice as many within the range of 100–200 μm from the neural tube (n = 74 experimental and 65 control cells analyzed from five separate experiments). We also noted a significant difference in both the total distance traveled (i.e., including the various turns made by the cells) and the net distance away from the neural tube of neural crest cells exposed to soluble Slit2 compared with control CM (Fig. 9, b and c). Accordingly, the net path length was 36% longer in the Slit2-exposed cells compared with control-treated length (38 ± 3 μm in Slit2 compared with 28 ± 3 μm in control medium, $P < 0.02$, Mann-Whitney test), as was the total path length (139 ± 15 μm for control and 167 ± 14 μm for Slit2, $P < 0.005$, Mann-Whitney test; Fig. 9 b). We analyzed the speed of movement in groups of cells assayed for similar lengths of time and found an average

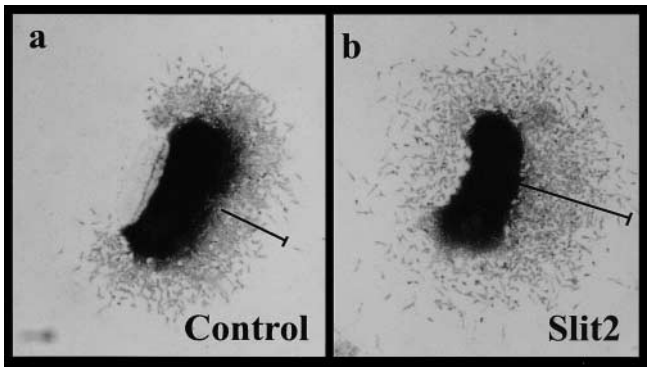

Figure 6. **Neural crest cells migrate further in the presence of Slit2 CM.** (a) A neural tube explanted in the presence of CM from control cells shows that migrating neural crest cells have moved several cell diameters away from the neural tube after 18 h in culture. (b) A similar neural tube cultured in medium conditioned by Slit2-expressing cells had neural crest cells that had migrated significantly further in 18 h.

Table III. **Slit2 enhances migration of trunk, not vagal, neural crest cells**

	Control	Slit2	
	μm	μm	
Trunk	133 ± 3.8	161 ± 4.2	21%[a]
Vagal	132 ± 7	125 ± 6	−6%

Neural tubes were cultured overnight on fibronectin. Values correspond to the average distance traveled by the neural crest cells away from the neural tube explant ± SEM. For trunk, there were a total of >100 neural tubes per condition in 12 separate experiments. For vagal, there were 12 neural tubes per condition in three separate experiments.
[a]$P < 0.0001$, t test.

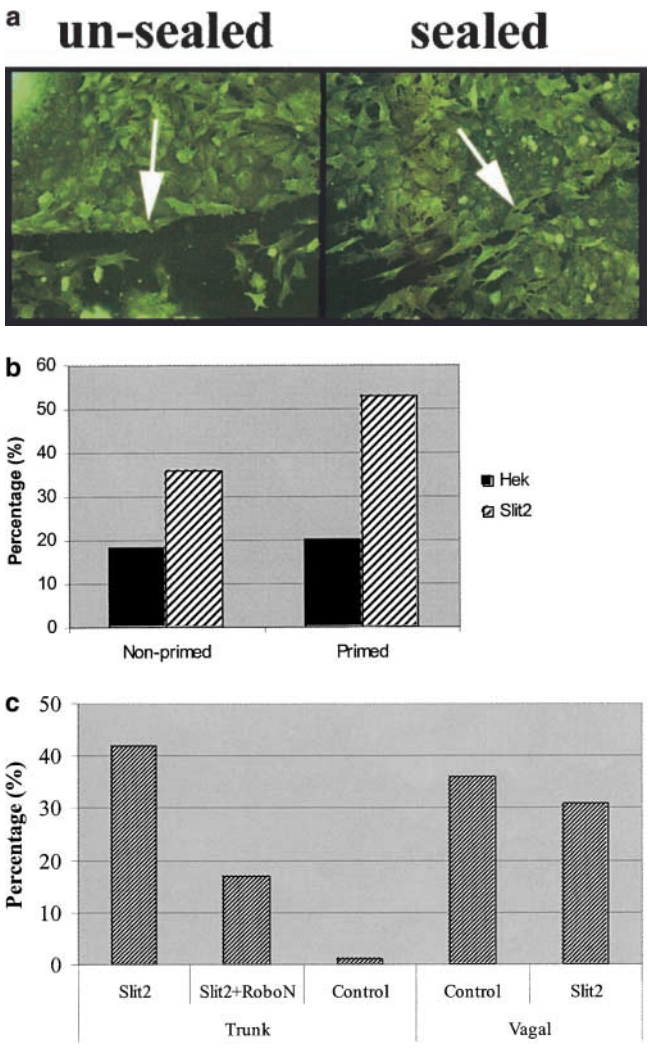

Figure 7. **Slit2 enhances trunk neural crest motility in a wound assay.** Trunk neural tubes were cultured overnight on fibronectin. After one day, media was changed to one conditioned by control or Slit2-secreting cells. A wound of one to two cells width was made with a fine pipette. After 2 h, the percent of wounds with cells crossing and sealing the gap was determined. (a, unsealed) Image of a neural crest culture fixed immediately after wounding and stained with the HNK-1 antibody. (a, sealed) Image of a similar culture fixed 4 h after wounding showing that many neural crest cells have sealed the gap by this time point. (b) Primed neural crest cultures were incubated for 2 h before performing the wound with media conditioned for 5 d by control HEK cells or Slit2-secreting cells. Nonprimed corresponds to neural crest cells that were not preexposed to Slit2 in the media before the wound. Data correspond to one representative experiment out of eight. (c) Slit2 enhances wound healing of trunk, not vagal, neural crest, and this effect can be reversed by soluble Robo. The enhanced migration of trunk neural crest by Slit2 was significantly reduced by the presence of RoboN in the media. Neural crest cultures were primed for 2 h before performing the wound with media conditioned for 5 d by control HEK cells, Slit2-secreting cells, or a 1:1 combination of RoboN and Slit2 media. After 2 h of culture, the percent of wounds with cells crossing and sealing the gap was determined. Data correspond to one representative experiment of six.

increase in speed of 52% in Slit2-containing medium relative to the control ($P < 0.009$, *t* test). Interestingly, the persistence and directionality were not significantly different between control and Slit2 exposed. Thus, the cells change directions with the same frequency but move further in the same time in the presence of Slit2.

Table IV. **Slit2 enhances wound closure by trunk, not vagal, neural crest cells**

	Percent of sealed wounds			
	Nonprimed	Primed		
	Trunk	Trunk	Trunk + RoboN	Vagal
Control	9 ± 4	13.8 ± 5.5	18 ± 3.8	8.7 ± 0.8
Slit2	22 ± 5	41.6 ± 5.6[a]	18 ± 1.5[b]	7.0 ± 1.7

Trunk neural tubes were cultured overnight on fibronectin. After one day, media was changed to one conditioned by control or Slit2-secreting cells. A wound of one to two cells width was made with a fine pipette. After 2 h, the percent of wounds with cells crossing and sealing the gap was determined. For trunk, there were a total of >100 neural tubes per condition in five or seven separate experiments (nonprimed and primed, respectively). For vagal, there were >70 neural tubes per condition in three separate experiments.
[a]$P < 0.005$, *t* test, in trunk exposed to control versus Slit2 media.
[b]$P < 0.02$, *t* test, in trunk exposed to Slit2 versus Slit2 + RoboN media.

Discussion

Neural crest cells arising from the vagal axial level form the enteric ganglia that innervate the gut. They invade the foregut and migrate long distances from rostral to caudal regions of the gut to populate its entire length. In contrast, trunk neural crest cells fail to invade gut tissue immediately below their migratory pathways. Even if transplanted to vagal levels, trunk neural crest cells do not enter the gut (Le Douarin and Teillet, 1973; Erickson and Goins, 2000). Several inhibitory molecules have recently been shown to play important roles in the general migratory process of neural crest cells, e.g., ephrinB family members, Semaphorin3A, and chondroitin sulfate proteoglycans (Oakley et al., 1994; Krull et al., 1997; Eickholt et al., 1999). Here, we show that substrate-bound Slit2 is a chemorepellent for migratory trunk, but not vagal, neural crest cells. The differential effects of Slit2 provide the first molecular explanation for the differences in the migratory properties of these two populations.

The expression of Slits in the mesentery is uniform throughout the rostrocaudal extent of the gut mesenchyme. Thus, the selective entry of vagal neural crest cells lies not in the distribution of the ligand but rather with expression of Slit receptors, Robo1 and Robo2, in different neural crest populations (Li et al., 1999; Holmes and Niswander, 2001; Vargesson et al., 2001). Migratory and condensing trunk neural crest cells express both Robo receptors, whereas neither receptor was detected on vagal neural crest. The absence of Robo receptors on vagal neural crest cells is consistent with their lack of response to Slit2. In previous publications that have examined the embryonic distribution of Robos, no expression on migrating neural crest cells was noted. By using higher resolution in situ hybridization and, in particular, in situs performed on tissue sections, we detected expression of both Robo1 and Robo2 on trunk neural crest cells. Not all of the HNK-1–positive cells expressed detectable levels of Robo receptors; it is possible that some of the migrating cells expressed levels of receptors that were below the sensitivity of this method. Consistent

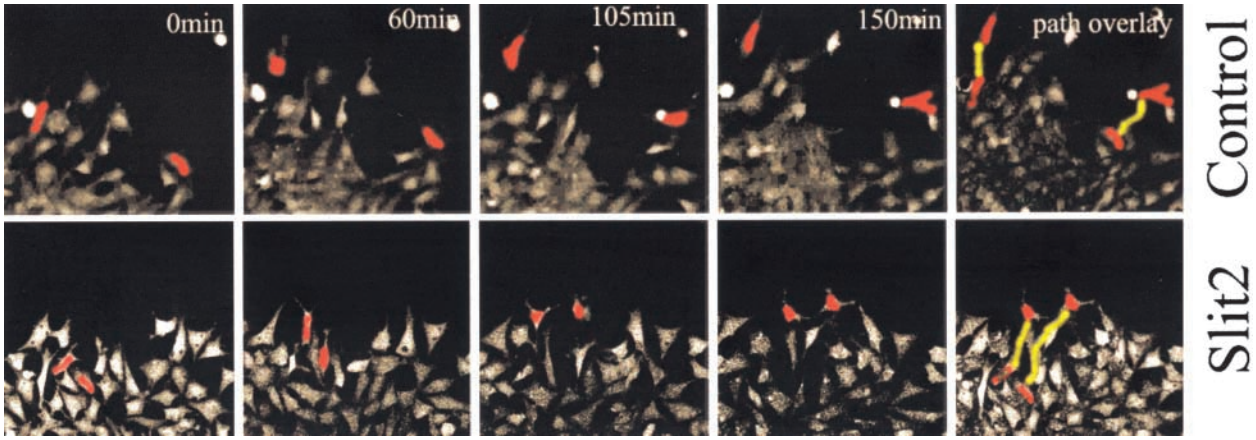

Figure 8. **Movie stills from time-lapse video microscopy.** Trunk neural crest cells exposed to Slit2 migrate further and have a longer total path length than those exposed to control medium. Trunk neural crest cells were labeled with Calcein AM (Molecular Probes) and washed before exposure to control or Slit2 CM. Cultures were time lapsed for ~2.5 h under a confocal microscope. Images represent stills from a movie taken at the indicated times. Two cells (red) in each movie were manually traced to follow their movements. Their final path length is indicated in yellow in the last frame.

with this possibility, older embryos during later stages of migration had more prominent Robo expression on migrating trunk neural crest cells, suggesting that receptor levels increase with developmental age.

Our data support the idea that Slits can function as direct chemorepellents for trunk neural crest cells. In vivo, we cannot rule out the possibility that Slits might also influence neural crest cells via indirect interactions with other tissues adjacent to neural crest migratory pathways, as the neural tube and dermomyotome also express Robo receptors. Our in vitro data, however, show that exogenous Slit2 and Slit1 can repel trunk neural crest cells in the absence of neighboring cell types. Furthermore, addition of RoboN specifically reverses the inhibitory effects of Slit2, suggesting a direct interaction.

Slit2 is likely not the only chemorepellent for trunk neural crest cells. Although Slit2 was used for most of the functional experiments performed here, we observed that multiple Slit

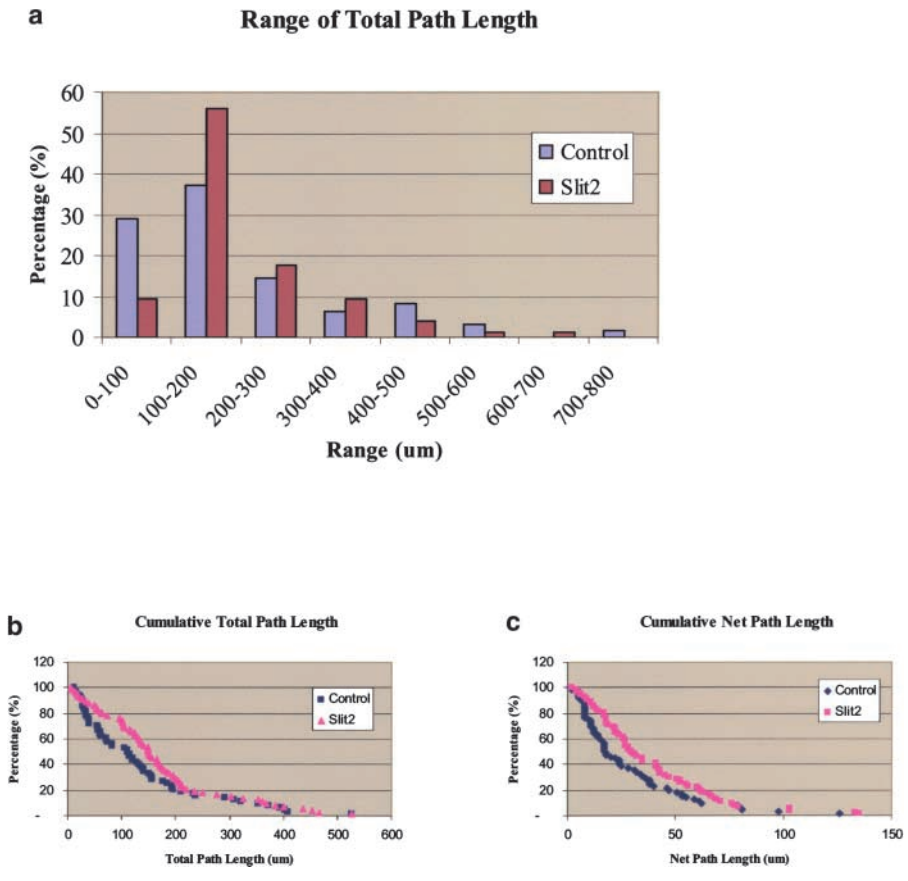

Figure 9. **Slit2 enhances neural crest cell migration.** Trunk neural crest cells exposed to Slit2 migrate for longer distances compared with control exposed neural crest cells. Trunk and vagal neural tubes were cultured overnight on fibronectin. After one day, media was changed to one conditioned by control or Slit2-secreting cells 1 h before video microscopy in a confocal microscope for 3 h. (a) The total path length was determined and normalized to a 2.5-h time period and binned in groups of 100-μm distances traveled. (b) Total path length (total distance traveled, including the various turns made by the cells) of neural crest cells was plotted as cumulative percentages of the distance traveled. (c) Net path length (net distance from starting point) of neural crest cells was plotted as cumulative percentages of the distance traveled.

isoforms, Slit1 and Slit3, have similar expression patterns in mesoderm at the entrance to the gut and that Slit1 can function similarly to Slit2. Furthermore, all three Slits share the highly conserved four leucine-rich repeats that have been shown to be responsible for Slit repellent activity (Battye et al., 2001; Chen et al., 2001; Nguyen Ba-Charvet et al., 2001a). Such redundancy has also been shown for olfactory neurons; these neurons that are repelled by endogenous Slit2 in the subventricular zone are also repelled by Slit1 (Wu et al., 1999). However, we cannot exclude the possibility that there are subtle functional differences in the different Slit proteins (Bagri et al., 2002; Plump et al., 2002).

The membrane-bound form appears to be responsible for Slit2's chemorepulsive effects on trunk neural crest cells. The 200-kD Slit2 glycoprotein is proteolytically processed into a 140-kD NH_2-terminal fragment and an ~60-kD COOH-terminal fragment in cell culture and in vivo (Brose et al., 1999; Nguyen-Ba-Charvet et al., 2001b). The NH_2 terminus is more tightly bound to the membrane and has been shown to mediate repellent activities and stimulation of axon elongation (Brose et al., 1999; Wang et al., 1999; Niclou et al., 2000; Battye et al., 2001; Nguyen-Ba-Charvet et al., 2001b). As the COOH terminus does not appear to interact with Robo receptors (Nguyen Ba-Charvet et al., 2001a), the repulsion we observed on neural crest cells almost certainly involves only the NH_2 terminus of the protein. In support of this, the leucine-rich repeats of the NH_2 terminus appear to be sufficient to achieve trunk neural crest repulsion (Chen et al., 2001; unpublished data). Moreover, trunk neural crest cells exposed to diffusible Slit2 either in chemotaxis chambers or collagen gels showed no apparent repulsion (unpublished data).

In addition to being a chemorepellent, our data suggest that soluble Slit2 selectively enhances the distance migrated by trunk neural crest cells. Such dual function for Slit2 concurs with observations on axon guidance where Slit family members have been shown to play multiple roles, causing both faster axon growth and induction of branching (Wang et al., 1999; Ozdinler and Erzurumlu, 2002). For the case of trunk neural crest cells, Slit2 appears to have opposite effects of inhibition and promotion of motility in the same cell type. Our results are consistent with previous studies showing that Slit2 can affect cell motility independent of its repulsive activity (Mason et al., 2001).

Although many trunk neural crest cells exhibited enhanced migration in the presence of soluble Slit2, a subpopulation of cells in explant cultures moved relatively short distances away from the center of the explant, as assayed both by static visualization and by time-lapse video microscopy. One possibility is that there are two separate populations of cells in our cultures. The majority (~90%) of cells was shown to be HNK-1–positive neural crest cells, but a minority population fails to express this epitope and may represent neural tube mesenchymal cells rather than neural crest cells. Thus, it is possible that this small population of Slit2-unresponsive cells represents a nonneural crest population.

The dual functions of Slit2 in both repulsion and stimulation of migration in the same type of cell are not necessarily contradictory; an optimal chemorepellent might logically be expected to stimulate rapid movement away from its source. Previous studies have shown that Slit2 repels axons from motor, olfactory, dentate gyrus, and retinal neurons (Brose et al., 1999; Li et al., 1999; Erskine et al., 2000; Ringstedt et al., 2000), while it inhibits migration of olfactory bulb and cerebral cortical neurons as well as leukocytes (Hu, 1999; Wu et al., 1999, 2001). In addition to repulsive effects on axonal growth and cell migration, Slit2 is a potent stimulator of axonal elongation and dendrite branching (Wang et al., 1999; Ozdinler and Erzurumlu, 2002; Whitford et al., 2002). In the last few years, several axonal pathfinding and axonal regeneration inhibitor molecules have been shown to induce both chemorepulsion or chemoattraction, depending on the type or age of the cell (Lohof et al., 1992; Song et al., 1998; Cai et al., 2001; Qiu et al., 2002). These opposing effects appear to be due to the internal levels of cyclic nucleotides in the cells, leading to promotion or inhibition of axonal growth (Cai et al., 1999; Hopker et al., 1999).

In summary, we have shown that Slit2 is a true bifunctional molecule: it can both repel neural crest cells and increase their rate of migration. The presence of Slit family members at the entrance of the gut mesenchyme coupled with the presence of Robo receptors on trunk and absence from vagal neural crest provides the first molecular explanation for the differences in migratory behavior of these two subpopulations via Slit chemorepulsion. The results suggest that neural crest cells may not only avoid, but also rapidly move away from, sources of chemorepellents like Slit.

Materials and methods

In situ hybridization

Embryos were removed from the eggs, stripped of membranes, and fixed in 4% paraformaldehyde overnight before being stored in 0.1 M PBS. Patterns of gene expression were determined by whole mount in situ hybridization using DIG-labeled RNA antisense probes as described by Henrique et al. (1995). The 1.7-kb c-slit1, 3.5-kb c-slit2, 1.9-kb cslit3, 1.9-kb c-robo1, and 2.1-kb c-robo2 (provided by E. Laufer, Columbia University, New York, NY) probes used are described in (Vargesson et al., 2001).

Section in situs were performed as follows. Embryos were fixed in modified Carnoy's and then dehydrated in 70%, 90%, 2 × 100% ethanol series, followed by two changes of histosol, and then paraffin. Sections were mounted on gelatin-covered superfrost glass slides and dried overnight. Before in situ, slides were dewaxed in histosol, rehydrated by passing through a series of ethanol (90, 70, and 50%), and rinsed in water, then PBS, and then in two changes of 2× SSC. Hybridization was done by diluting 1.5 ng/μl of slit2 and robo1 and 2 probes (Vargesson et al., 2001), incubated at 65°C overnight in 50% formamide, 2× SSC–humidified chamber. Slides were washed for 15 min in 50% formamide, 1× SSC, 0.1% Tween-20 at 65°C and then in MABT. The slides were then blocked for 1.5 h in MABT with 2% Boehringer blocking reagent and 20% any goat serum. Anti–DIG-AP was diluted 1:2,000 in the above solution and applied overnight at room temperature. The next day, slides were rinsed in MABT in agitated bath, 30 min each, and then equilibrated in NTMT (0.1 M NaCl, 0.1 M Tris, pH 9.5, 5 mM $MgCl_2$, 0.1% Tween-20) before BM purple color reaction.

In vivo avoidance assay

Fertilized eggs were incubated at 38°C for ~28–56 h, until embryos reached HH10–12 (for vagal neural crest) and HH12–16 (for trunk neural crest). Occasionally, stage 12 embryos received injections at both vagal and trunk levels. Eggs were windowed and visualized by a sub-blastodermal injection of India ink (diluted 1:10 in PBS). Slit2-expressing or control HEK293 cells, labeled with DiI, were injected in the somites at trunk or vagal levels. The eggs were closed with Scotch tape and reincubated for an additional 24 h. Embryos were removed from the eggs, stripped of the membranes, and fixed in 4% paraformaldehyde overnight before being stored in PBS. Embryos were thoroughly washed in PBS and then blocked overnight with PBS containing 1% Triton X-100 and 10% FBS at 4°C. After 3 h at room temperature in washing buffer (PBS with 1% Triton-X100, 1%

FBS), embryos were incubated with 1:300 HNK-1 supernatant in PBS overnight at 4°C. The next day, embryos were extensively washed and incubated with an anti–mouse IgM-specific Alexa 488–conjugated antibody (Molecular Probes). The next day, the embryos were washed extensively, Z scanned with a 410 LSM confocal microscope, and projected into a single file with LSM 5 Image Browser by Carl Zeiss MicroImaging, Inc.

In vitro avoidance assay

Quail neural tubes from HH10–12 (for vagal crest, using only the neural tubes from the first until the seventh somite) and HH13–16 (for trunk, the posterior parts of the tube) were dissociated in 1.5 mg/ml of dispase and washed in Leibovitz-15 medium. The neural tubes were cut in small pieces (size of two to three somites) and pipetted in the center of wells coated with fibronectin (10 μg/ml) already surrounded by a monolayer of live or dried Slit2 or control HEK293 cells (Li et al., 1999). Neural tubes were cultured in DME, 10% FBS, and 100 mg/ml and 100 U of penicillin and streptomycin, respectively, for 18 h, after which they were fixed in 4% paraformaldehyde for 30 min and subsequently blocked for 30 min with PBS, 1% Triton X-100, 10% FBS. Primary antibody was HNK-1 for visualizing neural crest cells, followed by an anti–mouse IgM–Alexa 488 secondary (Molecular Probes). At the end, slides were incubated with DAPI in PBS to visualize cell nuclei.

Neural crest response was determined as follows. If both types of cells (neural crest and HEK) either mixed and/or overlapped, it was scored as no repulsion. If, however, neural crest cells kept a marked distance between both cells, failed to overlap, and/or changed their shape from mesenchymal to slender, more collapsed, it was scored as repulsion. The number of neural tubes with such responses was counted, and the percentage was determined based on the total number of neural tubes with neural crest in close proximity to the control cells. Neural tubes with neural crest cells that were not in close proximity to the cells were not counted.

Transient transfections of mSlit1 (Wu et al., 1999) into HEK293 cells were done using Lipofectamine 2000™ (Invitrogen) according to the manufacturer's instructions. The next day, cells were lifted and plated onto fibronectin-coated slides overnight. The next day, a hole in the monolayer was created, neural tubes were added, and the rest was as described above.

In vitro migration assay

Quail neural tubes from HH10–12 (for vagal crest) and HH13–16 (for trunk, the posterior parts of the tube were obtained as described above) were cultured in DME/10% FBS in fibronectin-coated 24-transwells (Corning) above either Slit2 or control HEK cells or CM from the same cells. Cultures were grown overnight, and the next day, neural crest cells could be seen as a halo around the neural tubes. The cultures were fixed with ice-cold methanol for 20 min, cells were stained with toluidine blue, and the maximal distance of neural crest cell from the neural tube was measured and compared.

In vitro wound assay

Quail neural tubes from HH13–16 (for trunk, the posterior parts of the tube were obtained as mentioned above) were cultured in DME/10% FBS in a fibronectin-coated 2-well chamber slide (Nunc) overnight, and the medium was changed to one conditioned for 5 d by Slit2 or control cells. For the priming experiments, neural crest cells were preincubated with CM for 2 h before making the wounds. Wounds were made by scraping cells (two to three cells–width lanes) with a pulled glass needle, and lanes were scored over 1–1.5-h periods to count the cells crossing the wound space. The criteria used was to count the points at which the wound was sealed at any length of the wound lane (regardless of the number) as "sealed"; "nonsealed" was scored as the number of lanes that did not have cells contacting from the opposing sides of the wound.

Time-lapse video microscopy

Quail embryos stage 13–15 were electroporated with pCIG vector carrying the GFP marker (Megason and McMahon, 2002) with two pulses of 100 mV each. After 1–2 h in a 38°C incubator, neural tubes were isolated as described above and cultured on glass slides coated with fibronectin in DME/10% FBS. The next day, cells were primed for 1 h with control or Slit2 CM as before, and labeled cells were imaged using a Carl Zeiss MicroImaging, Inc. 410 LSM every 90 s for ~3 h. The average speed traveled by individual neural crest cells in control versus Slit2-containing medium was determined by comparing cells filmed on the same day during a set number of frames (each frame corresponding to 90 s). The captured images were converted into a QuickTime movie with NIH Image 3 and analyzed with the DIAS (Dynamic Image Analysis System; Solltech Inc.) program for cell tracking and measurements.

Online supplemental material

The supplemental material (Fig. S1 and Videos 1 and 2) is available at http://www.jcb.org/cgi/content/full/jcb.200301041/DC1. The movies show neural crest cells moving from three different experiments combined together for control and Slit2-exposed neural crest cells. The lapsed time is ~2.5 h.

We thank Scott Fraser for helpful comments on the manuscript, Martin Garcia-Castro and Sara Ahlgren for help in analyzing the data, and Gustavo Gomez, Vivian Lee, and Joanne Tan-Cabugao for technical support.

This work was supported in part by a postdoctoral fellowship to M.E. De Bellard from the National Multiple Sclerosis Society (FA 1383-A-1) and by a United States Public Health Service grant (HD-15527) to M. Bronner-Fraser.

Submitted: 13 January 2003
Revised: 11 June 2003
Accepted: 16 June 2003

References

Bagri, A., O. Marin, A.S. Plump, J. Mak, S.J. Pleasure, J.L. Rubenstein, and M. Tessier-Lavigne. 2002. Slit proteins prevent midline crossing and determine the dorsoventral position of major axonal pathways in the mammalian forebrain. *Neuron.* 33:233–248.

Battye, R., A. Stevens, R.L. Perry, and J.R. Jacobs. 2001. Repellent signaling by Slit requires the leucine-rich repeats. *J. Neurosci.* 21:4290–4298.

Bronner-Fraser, M. 1982. Analysis of neural crest migration and differentiation using a microinjection technique. *Int. J. Neurol.* 16-17:73–94.

Bronner-Fraser, M., and A.M. Cohen. 1980. Analysis of the neural crest ventral pathway using injected tracer cells. *Dev. Biol.* 77:130–141.

Bronner-Fraser, M., C.D. Stern, and S. Fraser. 1991. Analysis of neural crest cell lineage and migration. *J. Craniofac. Genet. Dev. Biol.* 11:214–222.

Brose, K., K.S. Bland, K.H. Wang, D. Arnott, W. Henzel, C.S. Goodman, M. Tessier-Lavigne, and T. Kidd. 1999. Slit proteins bind Robo receptors and have an evolutionarily conserved role in repulsive axon guidance. *Cell.* 96: 795–806.

Brown, C.B., L. Feiner, M.M. Lu, J. Li, X. Ma, A.L. Webber, L. Jia, J.A. Raper, and J.A. Epstein. 2001. PlexinA2 and semaphorin signaling during cardiac neural crest development. *Development.* 128:3071–3080.

Cai, D., Y. Shen, M. De Bellard, S. Tang, and M.T. Filbin. 1999. Prior exposure to neurotrophins blocks inhibition of axonal regeneration by MAG and myelin via a cAMP-dependent mechanism. *Neuron.* 22:89–101.

Cai, D., J. Qiu, Z. Cao, M. McAtee, B.S. Bregman, and M.T. Filbin. 2001. Neuronal cyclic AMP controls the developmental loss in ability of axons to regenerate. *J. Neurosci.* 21:4731–4739.

Chen, J.H., L. Wen, S. Dupuis, J.Y. Wu, and Y. Rao. 2001. The N-terminal leucine-rich regions in Slit are sufficient to repel olfactory bulb axons and subventricular zone neurons. *J. Neurosci.* 21:1548–1556.

Eickholt, B.J., S.L. Mackenzie, A. Graham, F.S. Walsh, and P. Doherty. 1999. Evidence for collapsin-1 functioning in the control of neural crest migration in both trunk and hindbrain regions. *Development.* 126:2181–2189.

Erickson, C.A., and T.L. Goins. 2000. Sacral neural crest cell migration to the gut is dependent upon the migratory environment and not cell-autonomous migratory properties. *Dev. Biol.* 219:79–97.

Erskine, L., S.E. Williams, K. Brose, T. Kidd, R.A. Rachel, C.S. Goodman, M. Tessier-Lavigne, and C.A. Mason. 2000. Retinal ganglion cell axon guidance in the mouse optic chiasm: expression and function of robos and slits. *J. Neurosci.* 20:4975–4982.

Feiner, L., A.L. Webber, C.B. Brown, M.M. Lu, L. Jia, P. Feinstein, P. Mombaerts, J.A. Epstein, and J.A. Raper. 2001. Targeted disruption of semaphorin 3C leads to persistent truncus arteriosus and aortic arch interruption. *Development.* 128:3061–3070.

Henrique, D., J. Adam, A. Myat, A. Chitnis, J. Lewis, and D. Ish-Horowicz. 1995. Expression of a Delta homologue in prospective neurons in the chick. *Nature.* 375:787–790.

Holmes, G., and L. Niswander. 2001. Expression of slit-2 and slit-3 during chick development. *Dev. Dyn.* 222:301–307.

Holmes, G.P., K. Negus, L. Burridge, S. Raman, E. Algar, T. Yamada, and M.H. Little. 1998. Distinct but overlapping expression patterns of two vertebrate slit homologs implies functional roles in CNS development and organogenesis. *Mech. Dev.* 79:57–72.

Hamburger, V., and H.L. Hamilton. 1951. A series of normal stages in the development of the chick embryo. *J. Morph.* 88:49–92.

Hopker, V.H., D. Shewan, M. Tessier-Lavigne, M. Poo, and C. Holt. 1999. Growth-cone attraction to netrin-1 is converted to repulsion by laminin-1. *Nature.* 401:69–73.

Hu, H. 1999. Chemorepulsion of neuronal migration by Slit2 in the developing mammalian forebrain. *Neuron.* 23:703–711.

Hu, H. 2001. Cell-surface heparan sulfate is involved in the repulsive guidance activities of Slit2 protein. *Nat. Neurosci.* 4:695–701.

Kidd, T., K.S. Bland, and C.S. Goodman. 1999. Slit is the midline repellent for the robo receptor in *Drosophila*. *Cell.* 96:785–794.

Kinrade, E.F., T. Brates, G. Tear, and A. Hidalgo. 2001. Roundabout signalling, cell contact and trophic support confine longitudinal glia and axons in the *Drosophila* CNS. *Development.* 128:207–216.

Krull, C.E., R. Lansford, N.W. Gale, A. Collazo, C. Marcelle, G.D. Yancopoulos, S.E. Fraser, and M. Bronner-Fraser. 1997. Interactions of Eph-related receptors and ligands confer rostrocaudal pattern to trunk neural crest migration. *Curr. Biol.* 7:571–580.

Kulesa, P.M., and S.E. Fraser. 1998. Neural crest cell dynamics revealed by time-lapse video microscopy of whole embryo chick explant cultures. *Dev. Biol.* 204:327–344.

Kulesa, P.M., and S.E. Fraser. 2000. In ovo time-lapse analysis of chick hindbrain neural crest cell migration shows cell interactions during migration to the branchial arches. *Development.* 127:1161–1172.

Le Douarin, N.M. 1986. Cell line segregation during peripheral nervous system ontogeny. *Science.* 231:1515–1522.

Le Douarin, N.M., and M.A. Teillet. 1973. The migration of neural crest cells to the wall of the digestive tract in avian embryo. *J. Embryol. Exp. Morphol.* 30: 31–48.

Le Douarin, N.M., and M.A. Teillet. 1974. Experimental analysis of the migration and differentiation of neuroblasts of the autonomic nervous system and of neuroectodermal mesenchymal derivatives, using a biological cell marking technique. *Dev. Biol.* 41:162–184.

Le Douarin, N.M., E. Dupin, A. Baroffio, and C. Dulac. 1992. New insights into the development of neural crest derivatives. *Int. Rev. Cytol.* 138:269–314.

Li, H.S., J.H. Chen, W. Wu, T. Fagaly, L. Zhou, W. Yuan, S. Dupuis, Z.H. Jiang, W. Nash, C. Gick, et al. 1999. Vertebrate slit, a secreted ligand for the transmembrane protein roundabout, is a repellent for olfactory bulb axons. *Cell.* 96:807–818.

Lohof, A.M., M. Quillan, Y. Dan, and M.M. Poo. 1992. Asymmetric modulation of cytosolic cAMP activity induces growth cone turning. *J. Neurosci.* 12: 1253–1261.

Mason, H.A., S. Ito, and G. Corfas. 2001. Extracellular signals that regulate the tangential migration of olfactory bulb neuronal precursors: inducers, inhibitors, and repellents. *J. Neurosci.* 21:7654–7663.

Megason, S.G., and A.P. McMahon. 2002. A mitogen gradient of dorsal midline Wnts organizes growth in the CNS. *Development.* 129:2087–2098.

Nguyen Ba-Charvet, K.T., K. Brose, V. Marillat, T. Kidd, C.S. Goodman, M. Tessier-Lavigne, C. Sotelo, and A. Chedotal. 1999. Slit2-mediated chemorepulsion and collapse of developing forebrain axons. *Neuron.* 22: 463–473.

Nguyen Ba-Charvet, K.T., K. Brose, L. Ma, K.H. Wang, V. Marillat, C. Sotelo, M. Tessier-Lavigne, and A. Chedotal. 2001a. Diversity and specificity of actions of Slit2 proteolytic fragments in axon guidance. *J. Neurosci.* 21:4281–4289.

Nguyen-Ba-Charvet, K.T., K. Brose, V. Marillat, C. Sotelo, M. Tessier-Lavigne, and A. Chedotal. 2001b. Sensory axon response to substrate-bound Slit2 is modulated by laminin and cyclic GMP. *Mol. Cell. Neurosci.* 17:1048–1058.

Niclou, S.P., L. Jia, and J.A. Raper. 2000. Slit2 is a repellent for retinal ganglion cell axons. *J. Neurosci.* 20:4962–4974.

Oakley, R.A., C.J. Lasky, C.A. Erickson, and K.W. Tosney. 1994. Glycoconjugates mark a transient barrier to neural crest migration in the chicken embryo. *Development.* 120:103–114.

Ozdinler, P.H., and R.S. Erzurumlu. 2002. Slit2, a branching-arborization factor for sensory axons in the mammalian CNS. *J. Neurosci.* 22:4540–4549.

Plump, A.S., L. Erskine, C. Sabatier, K. Brose, C.J. Epstein, C.S. Goodman, C.A. Mason, and M. Tessier-Lavigne. 2002. Slit1 and Slit2 cooperate to prevent premature midline crossing of retinal axons in the mouse visual system. *Neuron.* 33:219–232.

Qiu, J., D. Cai, H. Dai, M. McAtee, P.N. Hoffman, B.S. Bregman, and M.T. Filbin. 2002. Spinal axon regeneration induced by elevation of cyclic AMP. *Neuron.* 34:895–903.

Ringstedt, T., J.E. Braisted, K. Brose, T. Kidd, C. Goodman, M. Tessier-Lavigne, and D.D. O'Leary. 2000. Slit inhibition of retinal axon growth and its role in retinal axon pathfinding and innervation patterns in the diencephalon. *J. Neurosci.* 20:4983–4991.

Song, H., G. Ming, Z. He, M. Lehmann, L. McKerracher, M. Tessier-Lavigne, and M. Poo. 1998. Conversion of neuronal growth cone responses from repulsion to attraction by cyclic nucleotides. *Science.* 281:1515–1518.

Vargesson, N., V. Luria, I. Messina, L. Erskine, and E. Laufer. 2001. Expression patterns of Slit and Robo family members during vertebrate limb development. *Mech. Dev.* 106:175–180.

Wang, H.U., and D.J. Anderson. 1997. Eph family transmembrane ligands can mediate repulsive guidance of trunk neural crest migration and motor axon outgrowth. *Neuron.* 18:383–396.

Wang, K.H., K. Brose, D. Arnott, T. Kidd, C.S. Goodman, W. Henzel, and M. Tessier-Lavigne. 1999. Biochemical purification of a mammalian slit protein as a positive regulator of sensory axon elongation and branching. *Cell.* 96: 771–784.

Whitford, K.L., V. Marillat, E. Stein, C.S. Goodman, M. Tessier-Lavigne, A. Chedotal, and A. Ghosh. 2002. Regulation of cortical dendrite development by Slit-Robo interactions. *Neuron.* 33:47–61.

Wu, J.Y., L. Feng, H.T. Park, N. Havlioglu, L. Wen, H. Tang, K.B. Bacon, Z. Jiang, X. Zhang, and Y. Rao. 2001. The neuronal repellent Slit inhibits leukocyte chemotaxis induced by chemotactic factors. *Nature.* 410:948–952.

Wu, W., K. Wong, J. Chen, Z. Jiang, S. Dupuis, J.Y. Wu, and Y. Rao. 1999. Directional guidance of neuronal migration in the olfactory system by the protein Slit. *Nature.* 400:331–336.

Yuan, W., L. Zhou, J.H. Chen, J.Y. Wu, Y. Rao, and D.M. Ornitz. 1999. The mouse SLIT family: secreted ligands for ROBO expressed in patterns that suggest a role in morphogenesis and axon guidance. *Dev. Biol.* 212:290–306.

Zhu, Y., H. Li, L. Zhou, J.Y. Wu, and Y. Rao. 1999. Cellular and molecular guidance of GABAergic neuronal migration from an extracortical origin to the neocortex. *Neuron.* 23:473–485.